Condensed Matter Physics, 1998, Vol. 1, No 2(14), p. 213–238

Ab initio water hexamers and octamers: tool to study hydrogen-bonded pattern in liquid water

E.Kryachko [1,2,3]

[1] Bogolyubov Institute for Theoretical Physics, Kyiv-143, Ukraine 252143

[2] Cherry L. Emerson Center for Scientific Computation and Department of Chemistry Emory University, Atlanta, GA 30322, U. S. A.

[3] Department of Chemistry, The Johns Hopkins University, Baltimore, MD 21218, U. S. A.

Received March 18, 1998

Fourteen different structures of water hexamer found *ab initio* within a 6-311G** basis set in the interval of 1.7 kcal/mol above the global minimum represent an unprecedently wide range of conformational plasticity of liquid water. The present work also provides the first *ab initio* demonstration of the existence of pentacoordinated water clusters.

Key words: *liquid water, H-bond pattern, orientational defect, water cluster, "Dangling" bond, Ab initio HF 6-311** calculation*

PACS: *61.20.Ja, 61.25.Em, 61.20.Gy, 62.30.+d, 63.20.Pw, 63.90.+t, 64.70.Ja, 65.50.+m, 64.30.+t*

1. Introduction

Liquid water is the most mysterious substance for natural scientists because of its great importance in the Universe and its versatile abnormal properties are far from being completely understood. It is formed due to hydrogen or, shortly, H-bonds and it is, in fact, its H-bonded pattern with interconnectivity and tortuosity that always plays the role of the key starting point in numerous studies aimed at resolving water paradigm [1] (see also [2]).

It has been known for a long time that H-bonded patterns of liquid water and hexagonal ice Ih are tetrahedral [1(a)]. They were also believed to have much more similarities between them. That is why ice was often chosen as a reasonable reference model for the study of an H-bonded water pattern. The aforementioned tetrahedrality originates, in fact, from the tetrahedral charge distribution around

the oxygen atom in a water monomer possessing two positive partial charges at the positions of hydrogen atoms and two negative partial charges that refer to ear-like lone electron pair. This idea was expressed by Bernal-Fowler-Pauling and called ice rules [3]:
(i) There are exactly two hydrogen atoms that belong to each oxygen atom with the O-H bond length of 1 Å;
(ii) There is exactly one hydrogen atom that occupies each O$\cdots$O bond between any pair of neighbouring oxygen atoms.

What might an H-bonded pattern of liquid water be like then? Well, obviously, like ice. Its "icelikeness" is manifested in the fact that each oxygen atom is involved in two covalent and two hydrogen bonds, or equivalently, that each water molecule is four-bonded and is surrounded by four nearest-neighbour water molecules. The latter ones compose its first coordination shell. Within the Bernal-Fowler-Pauling H-bonded pattern, the oxygen atoms are arranged in such a way that all the O-O-O bond angles between the nearest-neighbour water molecules are tetrahedral, i. e., equal to circa 109.47^o. The hydrogen atoms decorate therein O-O "bonds", establishing the so-called "hydrogen bigamy".

Let us ask then the following question. Does this "icelikeness" adequately describe the whole H-bonded pattern of liquid water? Or, in other words. Does liquid water contain any "patches" in its pattern that in fact violate Bernal-Fowler-Pauling ice rules and are crucial for turning liquid water into what it actually is? The answers are certainly 'no' and 'yes', respectively. It is now apparently pretty hard to believe in resolving a liquid water paradigm denying the very existence of such non-icelikeness "patches". To put it simpler, water can be roughly described by a "two-state" model with one "state" obeying Bernal- Fowler-Pauling rules and another one violating them. The "two-state" model satisfies either the energetical or geometrical criterion imposed on the H-bonded pattern [4-6]. The former suggests that two water molecules are H-bonded if their interaction energy $V < V_{HB}$. The negative threshold H-binding energy V_{HB} plays the role of a model cutoff parameter. It is allowed to take on a sequence of values, $V_{HB} = -2n\varepsilon$ with integer n from interval $(10, 41)$ and $\varepsilon = 0.07575$ kcal/mol. V_{HB} varies then from - 6.2115 to - 1.5150 kcal/mol.

According to the geometrical criterion (for current references see [7]), two water molecules are H-bonded if the following three constraints are accomplished altogether. The first one is the constraint on interoxygen separations that must be less than R_{thr} = 3.5 - 3.7 Å [8]. R_{thr} determines the position of the first minimum of the g_{OO} radial distribution function and defines, in fact, the boundary of the first coordination shell. The second constraint is imposed on the distance between the oxygen atom of the acceptor water molecule and the hydrogen atom of the donor one. It should be smaller than $r_{thr} = 2.45$ Å, that is, the distance at which the first minimum of the radial distribution function g_{OH} takes place [8]. The third constraint limits angle δ_H between the participating oxygen, the hydrogen of the donor molecule and the oxygen atom of the acceptor molecule: $\delta_H > 160^o$. This constraint seems to be quite fragile and is often omitted because a reasonable deviation of δ_H from 160^o to smaller angles indicates a stronger nonlinearity of an H-bond. These constraints are sometimes supplemented by another one imposed on the values of the lone pair-oxygen-oxygen angle.

Regarding the O-O distribution function g_{OO} of liquid water at 25^o C [8], its first maximum is sharply peaked at 2.86 Å and its integral from zero to R_{thr}, which is interpreted as the mean number of water molecules within the first coordination shell, is about 4.5. This implies that the H-bonded pattern of liquid water partly possesses five-fold coordinated "patches". Their very existence unambiguously shows how far real liquid water is from that modelled by the Bernal-Fowler-Pauling rules. One may even insist that its natural perfection is, in fact, in its imperfection which makes water so anomalous and so mysterious for natural science. In terms of patterns, this imperfection might be explained by the fact that water possesses some sort of defects, namely, such "patches" in its H-bonded pattern where the Bernal-Fowler-Pauling rules are violated. It has been thought that these defects manifest themselves in many ways, for instance, in conductivity, in water restructuring resulting in a flow of water, in interpreting the Raman [9,10] and infrared spectra [1]. They are usually divided into two types: ionic and orientational, depending on which the Bernal-Fowler-Pauling ice rule is violated.

In the present work we focus only on orientational defects which represent the violation of the second Bernal-Fowler-Pauling rule. The simplest model of an orientational defect was a long time ago suggested by Bjerrum [11(a)] (see also [1]). The Bjerrum orientational defects are of two types. One corresponds to the "empty" O $\cdots$O bond and is called L-defect [11(b)]. Another one, D-defect [11(b)] is, in fact, a doubly occupied bond O - H $\cdots$ H - O. This definition of orientational defects is rather schematic and does not take into account the cooperative nature of H-bonding in liquid water. The progress towards understanding the nature of orientational defects was made due to the first and in some sense semi-empirical calculations by Dunitz [12(a)], Cohan et al. [12(b)], and Eisenberg and Coulson [12(c)] (see also [12(d-h)]). These calculations show that an orientational defect is actually some area of the H-bonded pattern around an "empty" or doubly occupied H-bond that should include some distorted H-bonds around. Distortion is primarily thought in terms of δ_H angle whose value in the range of $160^o - 130^o$ describes a leaned or nonlinear H- bond that converts to the so-called bifurcated H-bond when this angle approaches $120^o - 100^o$. A physical model of a solitonic-type orientational defect where the central part is, in fact, a sort of a bifurcated H-bond was elaborated in [13] (for recent review see [14]).

A bifurcated H-bond is such a specific type of H-bond where the hydrogen atom simultaneously participates in or donates two hydrogen bonds. In other words, the hydrogen atom is shared by a couple of oxygen atoms simultaneously [9]. It is believed that these bonds contribute significantly to the Raman [10] and infrared [1] (see also [13(b)]) spectra of liquid water. It is also believed that they are important in mobility of water molecules. This view was supported experimentally [15] and by computer simulations [16,17]. However, it should be stressed that all these Bjerrum-type defects rely on the tacit assumption of preserving a four-fold coordination. It has been recently suggested [17] that a five-fold "patch" is a new type of an orientational defect with a bifurcated H-bond which appears as a result of approaching the fifth water molecule (see also [10(b)]). As suggested in [17] as well, this "patch" facilitates a transition from one Bernal-Fowler-Pauling pattern to another through a lowered energy barrier. The similar model of a five-fold "patch" was discussed in [18]. There is still another very specific feature of liquid water worth mentioning. It is the O-O-O bond angle distribution function that, according to the recent studies [19] (see also [17(b), 18]), reveals two maxima. One corresponds to the tetrahedral bond angle. Another one, peaked at $\angle$O-O-O $= 60^o$, demonstrates that the corresponding water molecules are settled in nontetrahedral directions.

In this context, pentacoordinated "patches" within an H-bonded pattern of liquid water are an appealing concept, since they constitute a simple and, to some extent, a rather universal principle of the underlying liquid water dynamics. The aim of the present paper is to reveal such "patches" in water clusters by means of performing *ab initio* search over their total potential energy surfaces and to study the properties of these defects. Section II deals with the computational GAUSSIAN-type methodology of this work. The next Section III starts with a brief description of the present status of *ab initio* water clusters and continues with the exhaustive search of the total potential energy surface of water hexamer cluster to reveal novel lower-lying water hexamer structures and in particular those of hexamers and octamers that possess pentacoordinated "patches". This is, in fact, the first evidence of *ab initio* five-fold coordinated water clusters. Section VI discusses and summarizes the present work.

2. Computational methodology

All the calculations were performed with the Gaussian-94 suite of programs [20] at the Cherry L. Emerson Center for Scientific Computation of Emory University in Atlanta. The ground-state geometry of water clusters was optimized at the Hartree-Fock level of computation with the triply split valence 6-311G** basis set of 180 basis functions that includes polarization functions on the oxygen and hydrogen atoms in particular [21]. In all the computations, no constraints were imposed on the geometry of water clusters. Full geometrical optimization was performed for each water cluster structure, and the attainment of the energy minimum was verified by calculating the vibrational frequencies that result in the absence of negative eigenvalues. Default options were used for the SCF convergence and for the threshold limits determining the final changes in the maximum forces and displacements in the geometry optimization. Vibrational modes and the corresponding frequences are based on a harmonic force field. Empirical scaling factors were not used. For conciseness, the tables report only the most intensive infrared (IR) and Raman active bands for which IR intensity and Raman activity exceed 100 km/mol and 20 $\mathring{A}^4$/amu, respectively.

3. Pentacoordinated water clusters

3.1. Prelude: hexamer and octamer

Study of water clusters is one of promising ways to resolve the liquid water paradigm. It is trivial, on the one hand, that a larger cluster better mimics bulky water. On the other hand, it is also quite evident that a larger cluster possesses a richer potential energy surface picture. It is then a rather well-spread and reasonable belief that to grasp the water paradigm, it might be sufficient to study those water cluster structures that occupy lower-lying energy minima on the potential energy surface. Should we be confident with this belief? Apparently, 'yes', if among lower-lying water cluster structures there are, in particular, those with five-fold coordinated water molecules.

Hexamer and octamer water clusters were the subject of a number of *ab initio* studies [22,23]. It has been recently shown [22(d)] that at the HF/6-311G** level of the computational theory, the global minimum of the hexamer potential energy surface is attained by prism structure. There are also two lower-lying local minima, one of which, corresponding to the cyclic chair- type structure, is 0.84 kcal/mol. Another one occupied by the boat-like structure distances from the chair-type one by 1.08 kcal/mol. There is yet another global minimum found at the cage-like water hexamer cluster with 8 H-bonds [23(d-g)]. To resolve this controversy, we have done an exhaustive search of the landscape of the total potential energy surfaces of water hexamer. The result of this search is reported in table 1 for energy, zero-point vibration energy (ZPVE) enthalpy and entropy, and in table 2 – for rotational constants and the total dipole moment and are displayed in figure 1. As it is seen in figure 1, three prism structures of $(H_2O)_6$ are at the bottom of the total potential energy surface. Prism I occupies its global minimum, but two others lie very close, at 2.4 and 5.8 cm^{-1}, taking the zero-point vibration energy into account. Five cage-type structures are followed by them. They are shown in figure 2. Table 2 demonstrates a good agreement of rotational constants for cages calculated in the present work and reported in [23(g)]. Four lower-lying cages I - IV possess very particular geometries. Their interoxygen distances between O_3 and O_4 are 3.577, 3.577, 3.466, and 3.570 Å, respectively. This implies that according to the first geometrical constraint these are precisely "dangling" bonds because of the absence of a hydrogen atom between these oxygens. Furthermore, some O-O-O interbond angles move away from the tetrahedral values to lower angles. For example, in cage I, $\angle O_3 - O_{14} - O_4 = 75.86^o$; in cage II, $\angle O_3 - O_{14} - O_4 = 75.85^o$; in cage III, $\angle O_3 - O_{15} - O_4 = 70.99^o$; in cage IV, $\angle O_3 - O_{14} - O_4 = 75.49^o$; and finally, in cage VI, $\angle O_1 - O_{15} - O_4 = 75.52^o$. The cage structure of water hexamer mimics the basic unit of one of the high-density polymorphs of ice, ice VI (compare with [1(a)], figure 3.8).

Proceding to the next structures, it is worth mentioning that prism VI is exactly the one found in [22(d)] at the global minimum. It is interesting that the open prism structure shown in figure 3 with a very high dipole moment of 4.38 D appears in the present list of lower-lying structures of water hexamer. Another cage structure, cage VI displayed in figure 4, is followed by an open prism and also possesses a rather high dipole moment equal to 3.45 D. Chair- or ring-type structure with

Table 1. Energy, enthalpy H, entropy S, and zero-point vibrational energy ZPVE of lower-lying water hexamers.

Structure	- Energy +456 hartrees	ΔE kcal/mol	ZPVE kcal/mol	- Enthalpy +456 hartrees	ΔH kcal/mol	S cal/mol K
chair	0.356702756	2.3619426	99.85516	0.180874	1.708691	132.506
		0.7666526			0.113401	
cageVI	0.357035657	2.1530463	100.99548	0.180491	1.949024	121.942
		1.6980763			1.494054	
op. prism	0.357431391	1.9047220	100.74973	0.181046	1.600760	123.652
		1.2040020			0.900040	
prism IV	0.358047985	1.5178074	101.30789	0.181304	1.438864	119.300
		1.3752474			1.296304	
prism VI	0.358048203	1.5177980	101.30876	0.181303	1.439492	119.297
		1.3761080			1.297757	
prism V	0.358048107	1.5177308	101.30871	0.181303	1.439492	119.301
		1.3759908			1.297752	
cage V	0.358758406	1.0720161	101.01288	0.182218	0.865327	121.718
		0.6344461			0.427757	
cage IV	0.358944226	0.9554135	101.09977	0.182346	0.785006	121.111
		0.6047335			0.434326	
cage III	0.3590113236	0.9133095	101.10253	0.182410	0.744846	120.990
		0.5653895			0.396926	
cage II	0.359012959	0.9122833	101.10311	0.182409	0.745474	120.983
		0.5649433			0.398134	
cage I	0.359013050	0.9122262	101.09889	0.182410	0.744846	121.022
		0.5606662			0.393286	
prism III	0.360449222	0.0110239	101.45604	0.183583	0.008785	118.301
		0.0166139			0.014375	
prism II	0.360465772	0.0006388	101.45668	0.183591	0.003765	118.317
		0.0068688			0.009995	
prism I	0.360466790	0.0	101.45045	0.183597	0.0	118.347
		0.0			0.0	

a zero total dipole moment concludes the present list. Table 1 also reports the calculated thermodynamic properties of the aforementioned structures. As it is seen there, the chair structure is characterized by the highest entropy of 132.51 cal/mol T. Entropies of cage VI and the open prism are larger than those of the prism I structure. This implies that despite the fact that the latter is at the global minimum at T=0 K, the energy ordering might change with raising the temperature. In figure 5 we display a phase-like diagram of some water hexamer structures. It is seen that prism I remains at the global minimum at T ¡ 130 K. If T$\geqslant$ 130 K, the ring structure becomes the lowest one by free energy. At room temperature, cages I-IV compete with prism I. It is interesting that at T> 300 K the open prism becomes more energetically favourable than prism I.

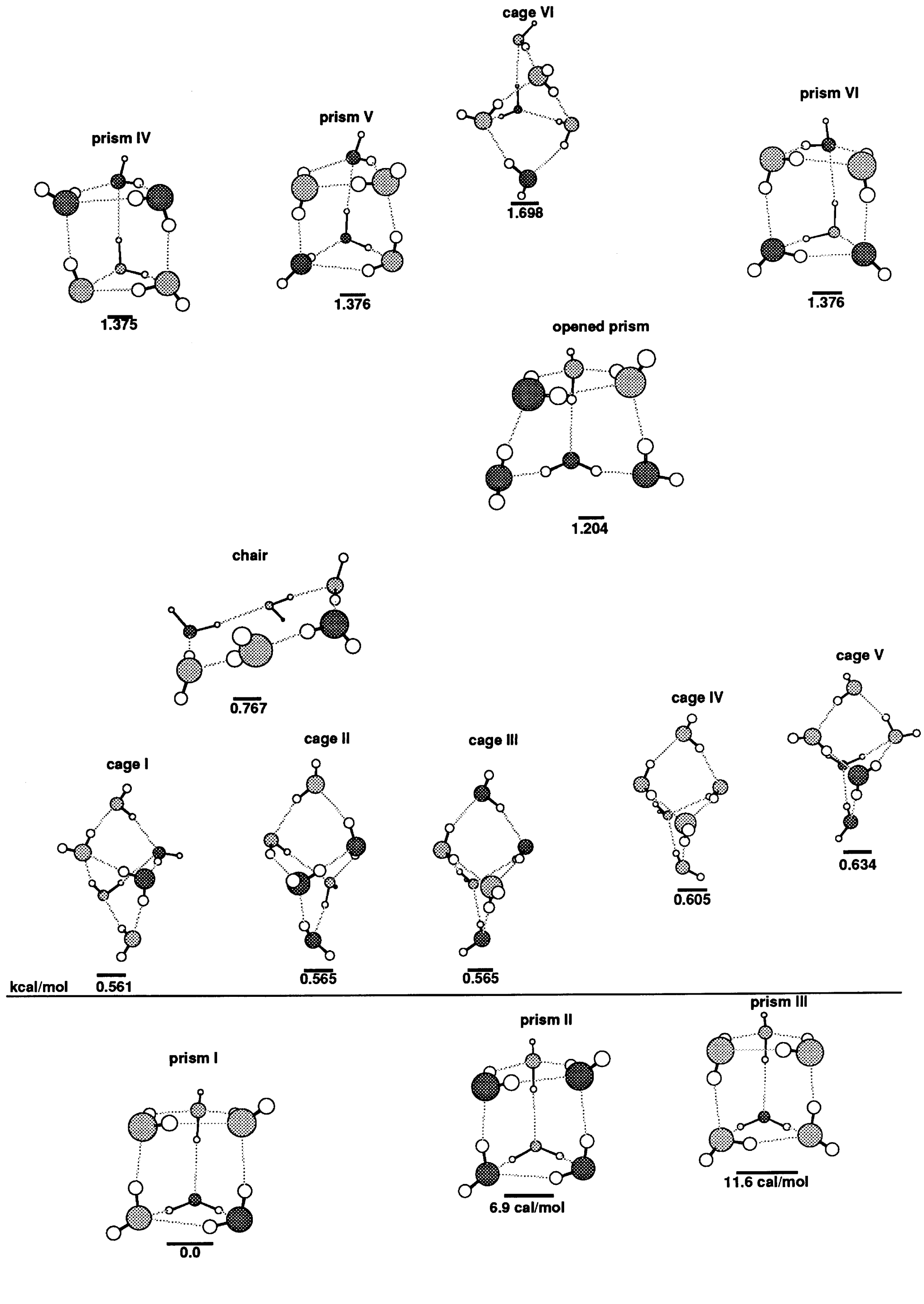

Figure 1. Lower-lying structures of water hexamer. In all figures O-H (solid line), H- (dashed), and "dangling" (dot-dashed) bonds.

Table 2. Rotational constants and total dipole moment of lower-lying water hexamer structures. Calculated rotational constants from [23(g)] are in parentheses.

Structure	Rotational constants, GHz			Dipole moment, D
chair	1.16607	1.16607	0.59509	0.0
cage VI	2.06059	1.08402	1.07861	3.4507
op. prism	1.57297	1.29319	1.07046	4.3841
prism IV	1.63253	1.28955	1.26493	2.8531
prism VI	1.63298	1.28948	1.26525	2.8512
prism V	1.63251	1.28955	1.26522	2.8523
cage V	2.11851	1.08603	1.02710	2.0095
cage IV	2.10894	1.09042	1.03060	2.0980
	(2.1334)	(1.1055)	(1.0790)	
cage III	2.13939	1.07922	1.01612	1.8585
	(2.1336)	(1.1021)	(1.0755)	
cage II	2.14024	1.07891	1.01597	1.8667
	(2.1341)	(1.1032)	(1.0754)	
cage I	2.13849	1.07943	1.01628	1.8524
	(2.1332)	(1.1027)	(1.0747)	
prism III	1.61272	1.32655	1.28996	2.9921
prism II	1.61462	1.32616	1.29057	2.9101
prism I	1.61452	1.32630	1.29033	2.9038

Table 3. Energy E, enthalpy H, entropy S, zero-point vibrational energy ZPVE, and free energy of defect water hexamer. Prisms I and VI and chair hexamers are chosen as the reference ones. $\Delta_{\text{prismI}} \equiv \Delta_o, \Delta_{\text{prismVI}} \equiv \Delta_p, \Delta_{\text{chair}} \equiv \Delta_c$. Δ_xX in kcal/mol, X = E, H, and G (at room T=298.15 K); Δ_x S in cal/mol K, $x = o, p, c$.

E (hartree)	H (hartree)	S (cal/mol K)	ZPVE (kcal/mol)
Δ_oE	Δ_oH	Δ_oS	Δ_oG
Δ_pE	Δ_pH	Δ_pS	Δ_pG
Δ_cE	Δ_cH	Δ_cS	Δ_cG
-456.3534556	-456.1773545	127.64111	100.24399
4.40	3.92	9.29	1.49
2.88	2.48	8.34	- 0.01
2.04	2.21	- 4.86	3.66

With regard to water octamer, it is well known that the cubic structure Ca [23(a)] of D_{2d} is the most stable one on the water octamer potential energy surface computed at the HF/6-311G** level. The cubic structure of S_4 symmetry occupies the local minimum that lies 3.49 kcal/mol above the Ca structure. In addition, there have been found another twenty five lower-lying octamer structures among which the ring structure R8a is energetically higher than the Ca one by 12.91 kcal/mol. At room temperature, their free energy difference diminishes to 0.19 kcal/mol [23(a)].

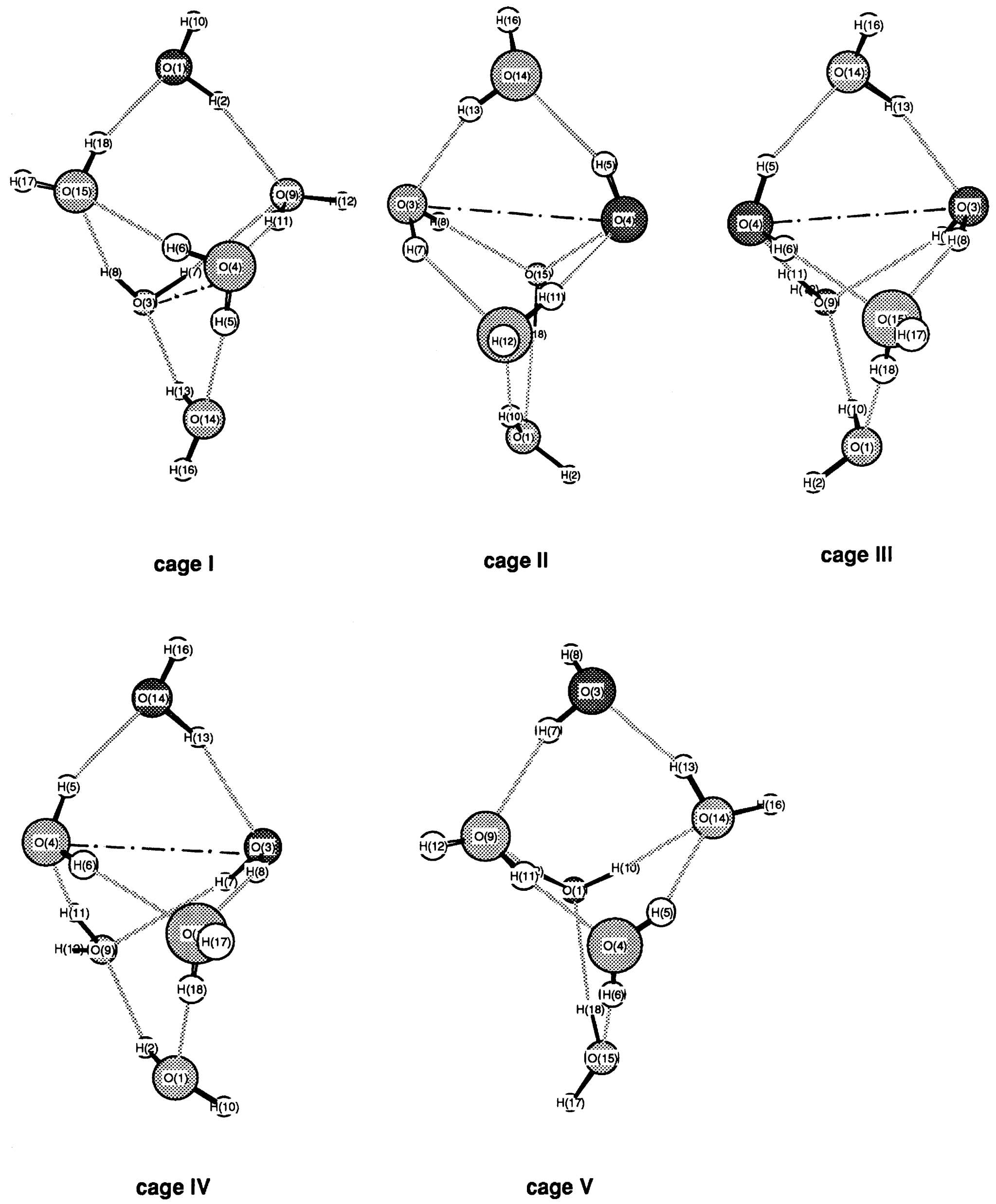

Figure 2. Five lowest cage structures of six molecules of water.

3.2. "Dangling" bond in water hexamer

A novel lower-energy local-minimum structure of $(H_2\,O)_6$ water cluster is revealed on the water hexamer potential energy surface at the HF/6-311G** level. It is shown in figure 6 and hereafter is named Defect I. Its total dipole is equal to 2.47 D. It lies above prism VI and chair water hexamers by 2.88 and 2.04 kcal/mol, respectively, and the distances from the prism I structure by 4.40 kcal/mol which reduces to 3.19 kcal/mol with taking ZPVE into account. The zero-point vibrational energy, enthalpy, free energy of Defect I and their differences with respect to the corresponding quantities for the prism and chair structures tabulated in [22(d)] are listed in table 3. One readily figures out that at room temperature, the energy of formation of Defect I is 1.49 kcal/mol with respect to that of prism I. It is worth mentioning that Defect I and prism VI are almost isoenergetical at room temperature (see also figure 7).

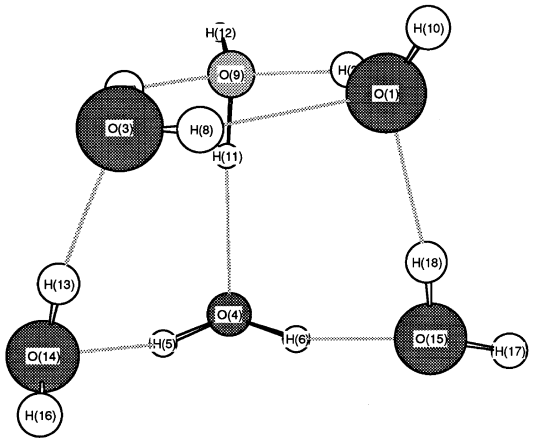

Figure 3. Opened prism water hexamer.

Internal coordinates of Defect I are presented in table 4. One sees there that in Defect I, water molecule $H_2H_3O_1$ distances from the nearest-neighbor water molecules with which it forms a covalent or H-bond rather different from the typical O-O separation of 2.86 Å inherent for the tetrahedral pattern. To specify, R(O_1 and O_4) = 2.93 Å, R(O_1 and O_5) = 3.08 Å, and R(O_1 and O_{15}) = 2.97 Å. Due to this, the water molecule has a fifth nearest-neighbour which is settled on the oxygen atom O_{10} and characterized by the distance R(O_1 and O_{10}) = 3.16 Å (see figure 6). The latter is less than R_{thr} and thus, one might think of these molecules as bonded to each other by the so-called "dangling" bond. One, therefore, concludes that this water cluster with a "dangling" bond is a five-folded "patch" that may appear among four-folded ones in an H-bonded

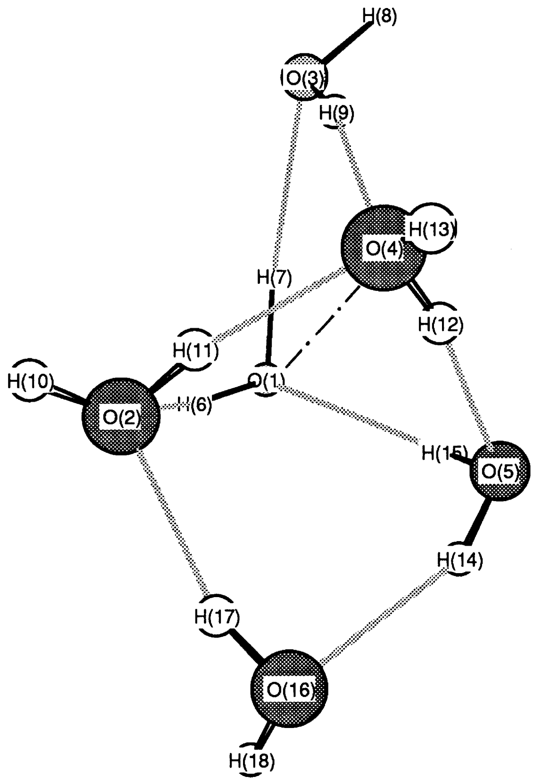

Figure 4. Cage VI cluster of six water molecules.

pattern of liquid water.

Table 4. Internal coordinates of defect water hexamer.

Interoxygen distance, Å			
$R(O_1-O_4)$	$R(O_1-O_5)$	$R(O_1-O_{10})$	$R(O_1-O_{15})$
	$R(O_4-O_{10})$	$R(O_4-O_{14})$	$R(O_4-O_{15})$
	$R(O_5-O_{10})$	$R(O_5-O_{14})$	$R(O_{10}-O_{14})$
2.932	3.075	3.162	2.969
	2.842	2.824	2.897
	2.953	2.869	4.120
H-bond length, Å			
$r(O_1-H_9)$	$r(O_1-H_{18})$	$r(O_4-H_3)$	$r(O_4-H_{11})$
$r(O_5-H_{13})$	$r(O_{10}-H_8)$	$r(O_{14}-H_6)$	$r(O_{15}-H_7)$
2.337	2.171	1.997	1.960
1.949	2.070	1.931	2.074
H-bond angle δ_H, deg			
$O_1-H_3-O_4$	$O_1-H_9-O_5$	$O_1-H_{18}-O_{15}$	$O_4-H_6-O_{14}$
$O_4-H_7-O_{15}$	$O_5-H_8-O_{10}$	$O_{10}-H_{11}-O_4$	$O_{14}-H_{13}-O_5$
167.99	134.63	141.29	155.45
144.44	154.30	153.55	161.84
O-O-O bond angle, deg			
$O_4-O_1-O_{15}$	$O_{10}-O_1-O_{15}$	$O_5-O_1-O_{15}$	$O_{14}-O_4-O_{15}$
	$O_1-O_4-O_{15}$	$O_{10}-O_5-O_{14}$	$O_1-O_5-O_{10}$
	$O_{10}-O_5-O_{14}$	$O_4-O_{14}-O_5$	$O_1-O_{15}-O_4$
62.75	43.89	87.60	73.37
	59.57	86.70	93.11
	86.70	63.41	57.67

Formation of a “dangling” bond promotes the appearance of nonlinear H-bonds between O_1, on the one hand, and O_5 and O_{15}, on the other one, with r (O_1-H_9) = 2.34 Å, $\angle O_1-H_9-O_5 = 134.63^o$, r $(O_1-H_{18}) = 2.17$ Å, and $\angle O_1-H_{18}-O_{15} = 141.29^o$. This is clearly seen in figure 6. It follows from table 4 that the “dangling” bond causes distortion of the rest of an H-bonded pattern of Defect I water hexamer that remains four-folded. For instance, R(O_5 and O_{10}) = 2.95 Å, r $(O_{10}-H_8)$ = 2.07 Å, $\angle O_5-H_8-O_{10} = 154.30^o$, and R($O_4$ and O_{15}) = 2.90 Å, r (O_4-H_{18}) = 2.07 Å, $\angle O_4-H_7-O_{15} = 144.44^o$. It should be noted that some O-O-O bond angles are clustered around 60^o. These are, in particular, the following: $\angle O_4-O_1-O_{15} = 62.75^o, \angle O_1-O_4-O_{15} = 59.57^o$, and $\angle O_4-O_{14}-O_5 = 63.41^o$. One also sees from table 4 that the lone-pair distribution of O_1 loses its tetrahedrality characterized by $\angle O_5-O_1-O_{15} = 87.60^o$ due to the five-fold coordination. We would like to conclude this paragraph by noting that due to the “dangling” bond, the separation between the oxygen atoms O_1 and O_{14} considered as second-neighbours is 4.22 Å.

The assignment of harmonic vibrations of the Defect I "patch" is shown in table 5. Harmonic frequencies computed for inter- and intra-molecular modes of the Defect I structure are listed in the second column of this table. Its third and fourth columns report the corresponding theoretical IR intensity and Raman activity. First of all, before studying table 5, it should be mentioned that the theoretical spectra of the chair and boat water hexamers [22(d)] do not have vibrations in the range 4000-4200 cm^{-1}. It implies that the hydrogen atoms in these structures are solely of two sorts: the hydrogens involved in forming H-bond, and "free" hydrogens participating in unbonded OH groups. On the contrary, the prism hexamers and Defect I do have H-stretching vibrations in this region. The most intensive IR band of Defect I is the librational one centered at 663.5 (IR intensity 564 km/mol, Raman activity 0.5 Å^4/amu) comparing with the most IR intensive ones for the prism, chair, and boat hexamers that fall into the region of H-stretching vibrations. The band at 663.5 cm^{-1} is assigned to the composed libration of the $O_4 - H_6$, $O_5 - H_8$, and $O_5 - H_9$ bonds. Other IR intensive bands of Defect I are the following: band 467.2 cm^{-1} (343.3, 2.2) associated with the composed librational vibration of $O_1 - H_3$, $O_5 - H_8$, $O_5 - H_9$, and $O_{15} - H_{18}$ bonds and others belong to the H-stretching region. These are band-centered at 4001.96 cm^{-1} (511.8, 22.0) with the $O_4 - H_6$, $O_{14} - H_{13}$ stretching vibration character and the band at 4111.4 cm^{-1} (369.8, 21.3) assigned merely to $O_4 - H_7$ stretching. Regarding the O-H stretching vibrational modes with the frequencies $\nu_1^{\text{theor}} = 4141.9$ cm^{-1} (17.7, 65.5; symmetric) and $\nu_3^{\text{theor}} = 4237.6$ cm^{-1} (57.4, 32.4; asymmetric) computed for the

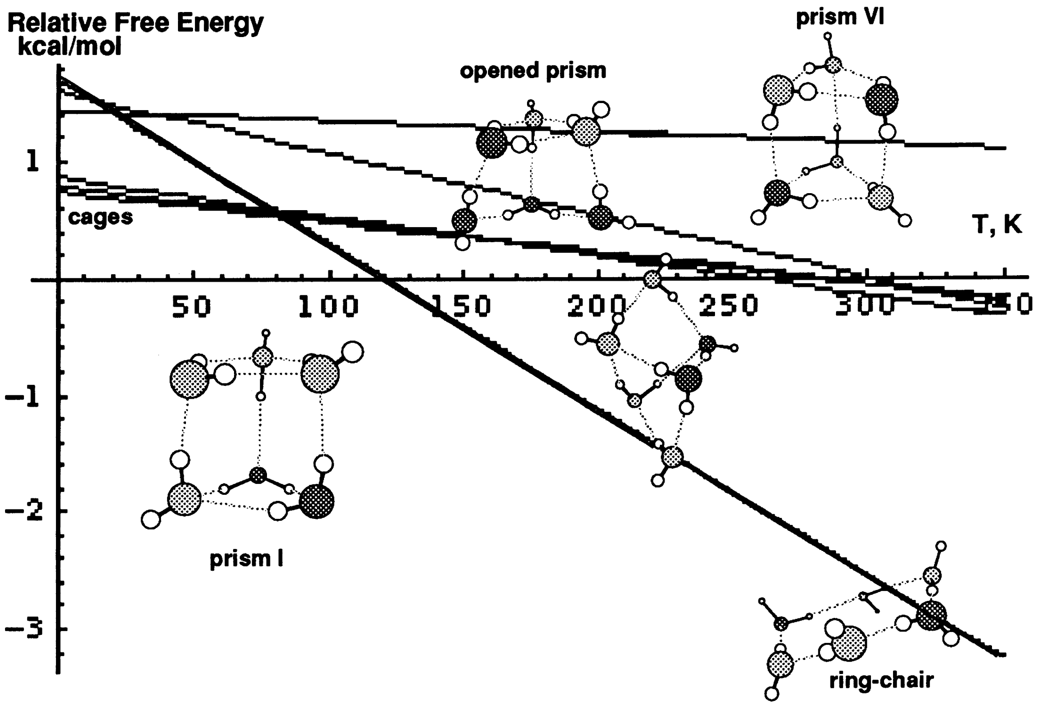

Figure 5. Phase-like diagram of lower-lying water hexamer clusters.

Table 5. Most intensive bands of Defect I water hexamer: vibrational frequencies ν, cm^{-1}, IR intensity (km/mol), Raman activity ($\mathrm{\AA}^4$/amu), force constant (mdyne/Å), and reduced mass (amu).

No.	ν cm^{-1}	IR intensity	Raman activity	Force constant	Reduced mass Assignment
1	96.52	131.68	2.08	0.0068	1.2344 $O_{15}-H_{17}$ translation
2	174.06	124.45	2.47	0.0251	1.4086 $O_{14}-H_{16}$ translation
3	220.78	108.64	1.34	0.0329	1.1462 $O_{10}-H_{12}$ translation
4	352.05	122.04	0.71	0.0761	1.0421 $O_1-H_2, O_5-H_8-H_9, O_{10}-H_{12}$ libration
5	426.87	191.66	1.32	0.1163	1.0830 $O_1-H_2, O_{15}-H_{17}-H_{18}$ libration
6	450.08	103.90	0.47	0.1293	1.0830 $O_1-H_2-H_3, O_5-H_9, O_{10}-H_{11}$ $-H_{12}, O_{15}-H_{18}$ libration
7	467.16	343.34	2.20	0.1357	1.0554 $O_1-H_3, O_5-H_8-H_9, O_{15}-H_{18}$ libration
8	591.19	203.24	4.31	0.2162	1.0497 O_1-H_3, O_4-H_7 libration
9	663.51	564.12	0.47	0.2763	1.0651 $O_4-H_6, O_5-H_8-H_9$ libration
10	750.18	102.25	0.41	0.3462	1.0442 $O_4-H_7, O_5-H_8, O_{10}-H_{11}$ libration
11	792.43	292.40	0.88	0.3940	1.0650 $O_4-H_6-H_7, O_5-H_9, O_{14}-H_{13}$ libration
12	913.97	112.38	0.88	0.5155	1.0475 $O_1-H_3, O_4-H_6-H_7$ libration
13	1756.83	203.58	3.66	1.9633	1.0797 $H_2-O_1-H_3, H_{11}-O_{10}-H_{12}$, $H_{17}-O_{15}-H_{18}$ scissor
14	1822.21	107.83	3.87	2.1091	1.0781 $H_2-O_1-H_3, H_8-O_5-H_9$ scissor
15	3967.47	79.66	162.57	9.7897	1.0566 $O_4-H_6, O_{14}-H_{13}$ stretch
16	4001.96	511.76	22.01	9.9429	1.0537 $O_4-H_6, O_4-H_7, O_{14}-H_{13}$ stretch
17	4016.36	167.01	25.95	10.0461	1.0570 $O_{10}-H_{11}$ stretch

Table 5. Continued from the previous page.

18	4047.50	227.75	89.05	10.1860	1.0553
					$O_1 - H_3, O_4 - H_6, O_{10} - H_{11}$ stretch
19	4068.80	143.11	36.64	10.2569	1.0516
					$O_5 - H_8, O_5 - H_9$ stretch
20	4085.39	211.26	48.75	10.3511	1.0526
					$O_{15} - H_{17}, O_{15} - H_{18}$ stretch
21	4111.36	369.79	21.25	10.7142	1.0758
					$O_4 - H_7$ stretch
22	4159.71	177.57	29.98	10.9754	1.0766
					$O_5 - H_9$ stretch
23	4183.20	111.31	32.23	11.0601	1.0727
					$O_1 - H_2$ stretch
24	4210.83	124.08	51.80	11.2187	1.0739
					$O_{10} - H_{12}$ stretch
25	4212.04	81.71	59.75	11.2060	1.0721
					$O_{14} - H_{16}$ stretch
26	4220.61	113.57	47.29	11.3126	1.0779
					$O_{15} - H_{17}$ stretch

HF/6-311 G** water monomer (for comments see [24]), one may divide the whole stretching region of Defect I into three groupings. The first one spans the range

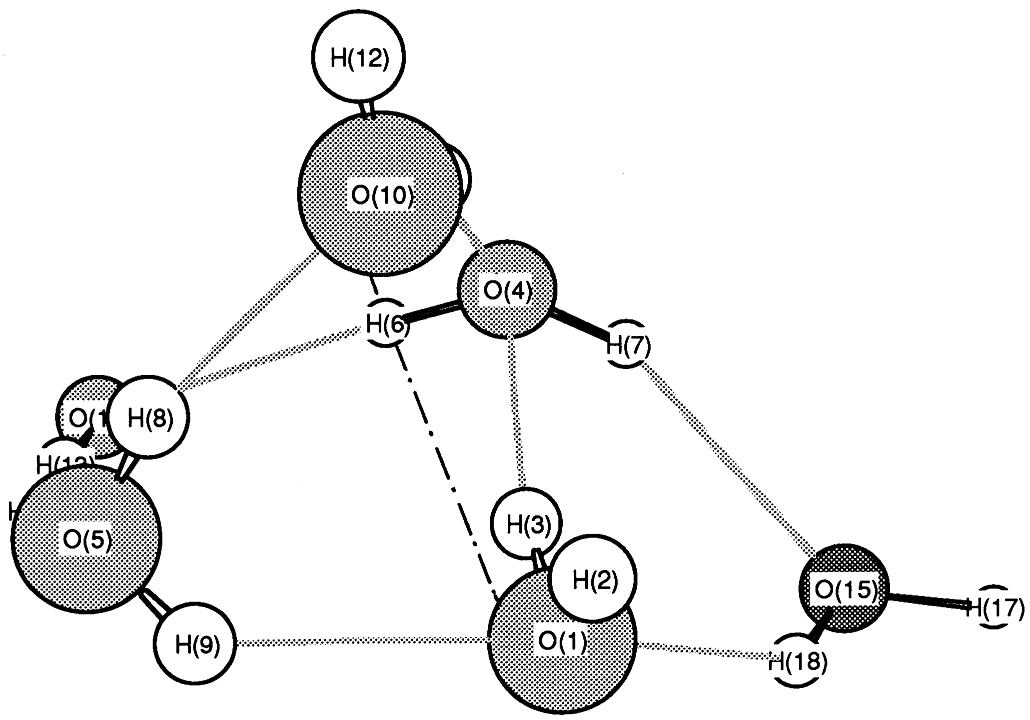

Figure 6. Pentacoordinated water hexamer cluster Defect I.

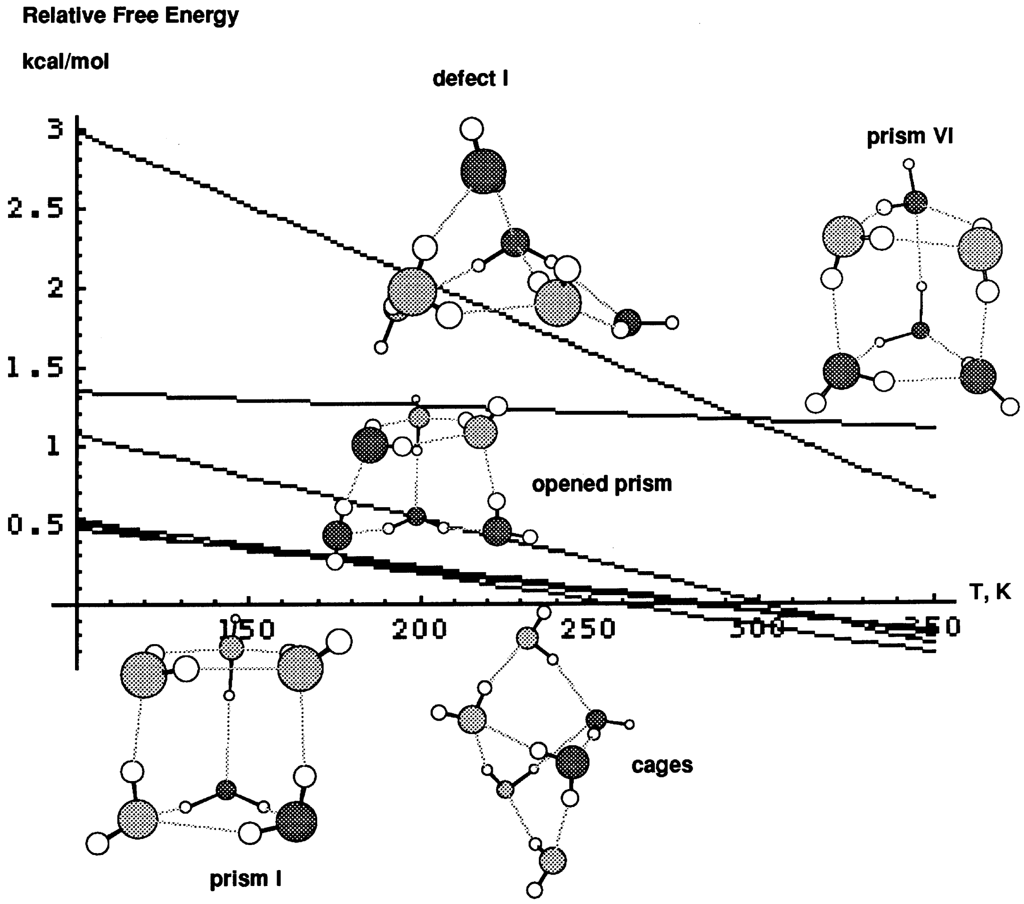

Figure 7. Phase-like diagram of Defect I and some lower-lying water hexamers.

from 3967 to 4069 cm^{-1} and possesses the dominant character of stretching the H-bonded hydrogen atoms. The band 3967.5 cm^{-1} (79.7; 162.6) describes the composed symmetric stretching vibration of $O_4 - H_6$, $O_{14} - H_{13}$ bonds and is, in fact, the strongest Raman active one. The aforementioned band 4002.0 cm^{-1} corresponds to asymmetric stretching vibration. Comparing with the stretching bands of a single water molecule, the latter are both redshifted, considerably enhanced, and become closer to each other by 60 cm^{-1}. The second grouping of bands lies in the interval from 4085 to 4180 cm^{-1} and is primarily contributed by nonlinear or bent H-bonded hydrogens. The last one consists of bands from 4183 to 4221 cm^{-1}. They are assigned to the stretching vibrations of "free" hydrogen atoms. These bands are slightly blueshifted and mainly twice enhanced comparing with the stretching mode ν_3 of a water monomer. Regarding the intramolecular or scissor modes of our defect hexamer structure, it has to be mentioned first that the harmonic mode $\nu_2^{(\mathrm{monomer})}$ of a water monomer calculated at the HF/6- 311G** level is 1750.3 cm^{-1}. Its IR absorption and Raman activity constitute 79.2 km/mol and 6.4 $\mathrm{\AA}^4$/amu, respectively. Two intra-molecular modes of Defect I are redshifted comparing with $\nu_2^{(\mathrm{monomer})}$ and more pronounced. Their normal vibration assignment is also shown. For instance, the first intramolecular mode of Defect I with frequency 1756.8 cm^{-1} describes the composed scissor vibrations of water molecules $H_2H_3O_1$ and $H_{11}H_{12}O_{10}$ bonded to each other via a "dangling" bond.

3.3. Five-fold coordinated water octamers

Figure 8 displays a pentacoordinated water octamer. Its distinction is that it has formed 3 H-bonds and looks identical to the structure R6c found in [23(a)], although a slight deviation in their properies is revealed [25]. Energy, enthalpy,

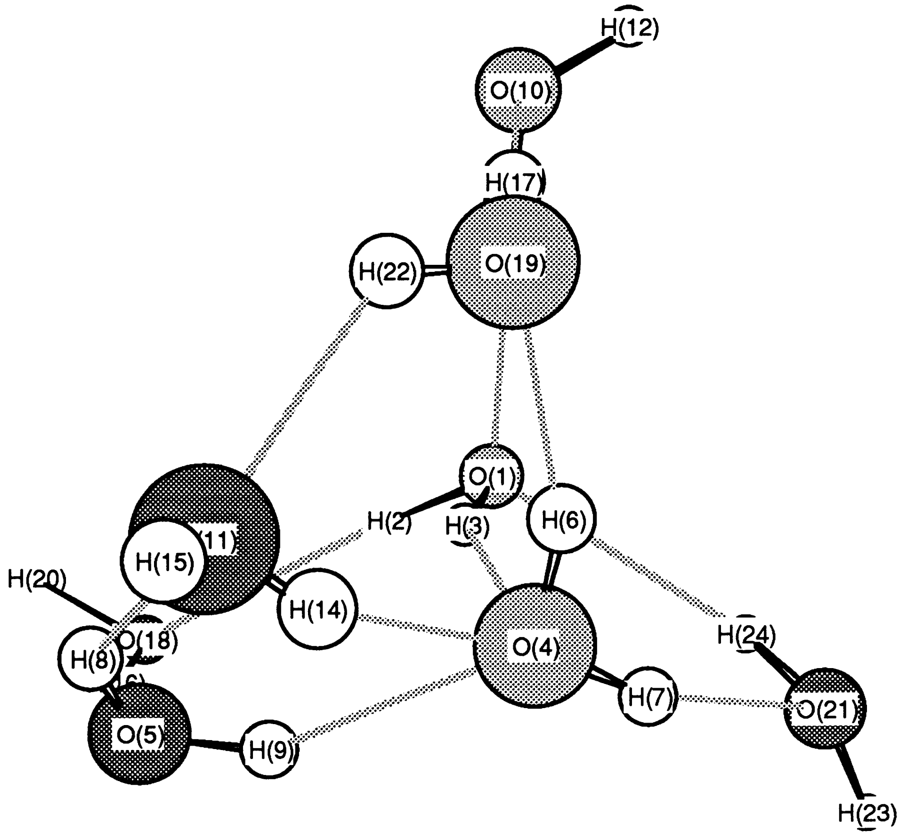

Figure 8. Pentacoordinated water octamer cluster Defect II.

zero-point vibrational energy and entropy calculated at the HF/6-311G** level of the computational theory of the octamer are reported in table 6. Before going further, one more word about the studied water clusters should be added. As to the cages and Defect I, they serve as examples in lower-lying clusters. Water molecule may form a first coordination shell with five water molecules in such

Table 6. Energy E, enthalpy H, entropy S, zero-point vibrational energy ZPVE, and free energy of defect water octamer. Cubic octamer Ca is chosen as the reference one. For other notations see caption of table 3.

Defect	E (hartree) Δ_{ca}E	H (hartree) Δ_{ca}H	S (cal/mol K) Δ_{ca}S	ZPVE (kcal/mol) Δ_{ca}G
Defect II	-608.4765824 12.291	- 608.2403860 10.802	156.181 17.905	134.42923 5.47

a way that the approaching fifth water molecule is bonded to the central water molecule by a "dangling" bond. Defect II portrayed in figure 8 is referred to an absolutely different type of pentacoordinated water clusters. It is seen there that the oxygen atom O_4 has three elongated and rather weak H-bonds with the oxygen atoms O_1, O_5, and O_{11} separated from it by circa 3 Å (table 7). Despite the fact that the angle $\angle H_6 - O_5 - H_7 = 107.13^o$ remains unchanged comparing with the water monomer. However, the lone-pair angular distribution suffers drastic changes, which is revealed in the calculated values of the corresponding angles: $\angle H_3 - O_4 - H_9 = 69.19^o$, $\angle H_9 - O_4 - H_{14} = 70.54^o$, and $\angle H_3 - O_4 - O_{14} = 115.65^o$. Its arrangement relative to the $H_6 - O_4 - H_7$ plane is determined by the anlges $\angle H_3 - O_4 - H_7 = 88.91^o$, $\angle H_6 - O_4 - H_{14} = 79.56^o$, and $\angle H_6 - O_4 - H_9 = 125.61^o$.

Table 7. Internal coordinates of defect water octamer.

Interoxygen distance, Å			
$R(O_1 - O_4)$	$R(O_1 - O_{10})$	$R(O_1 - O_{18})$	$R(O_1 - O_{21})$
$R(O_4 - O_5)$	$R(O_4 - O_{11})$	$R(O_4 - O_{19})$	$R(O_4 - O_{21})$
$R(O_5 - O_{11})$	$R(O_5 - O_{18})$	$R(O_{10} - O_{19})$	$R(O_{11} - O_{19})$
3.051	2.883	2.842	2.930
2.989	2.972	2.802	2.890
2.990	2.862	2.875	3.061
H-bond length, Å			
$r(O_1 - H_{13})$	$r(O_1 - H_{24})$	$r(O_4 - H_3)$	$r(O_4 - H_9)$
$r(O_4 - H_{14})$	$r(O_5 - H_{16})$	$r(O_{10} - H_{17})$	$r(O_{11} - H_8)$
$r(O_{11} - H_{22})$	$r(O_{18} - H_2)$	$r(O_{19} - H_6)$	$r(O_{21} - H_7)$
1.965	2.086	2.164	2.120
2.207	1.948	1.955	2.238
2.370	1.941	1.892	2.051
H-bond angle δ_H, deg			
$O_1 - H_3 - O_4$	$O_4 - H_9 - O_5$	$O_5 - H_8 - O_{11}$	$O_1 - H_{13} - O_{10}$
$O_4 - H_{14} - O_{10}$	$O_1 - H_2 - O_{18}$	$O_5 - H_{16} - O_{18}$	$O_4 - H_6 - O_{19}$
$O_{10} - H_{17} - O_{19}$	$O_4 - H_7 - O_{21}$	$O_{11} - H_{22} - O_{19}$	$O_1 - H_{24} - O_{21}$
155.49	152.07	136.03	161.78
137.24	157.20	160.34	158.87
162.59	146.57	129.83	147.54
O-O-O bond angle, deg			
$O_1 - O_{18} - O_5$	$O_4 - O_5 - O_{18}$	$O_{10} - O_1 - O_{18}$	$O_{11} - O_5 - O_{18}$
$O_5 - O_4 - O_{19}$	$O_1 - O_{10} - O_{19}$	$O_4 - O_{19} - O_{10}$	$O_{11} - O_4 - O_{19}$
	$O_5 - O_4 - O_{21}$	$O_{10} - O_1 - O_{21}$	$O_{11} - O_4 - O_{21}$
		$O_{18} - O_1 - O_{21}$	$O_{19} - O_4 - O_{21}$
77.73	104.14	122.58	138.43
103.22	84.15	99.21	63.95
	113.46	112.69	169.30
		122.74	111.81

Being a Ca structure, Defect II possesses 12 H-bonds albeit 7 of which may be considered relatively weak because their lengths exceed 2 Å. What is most impressing in the H-bonded pattern of Defect II is that water molecule $H_{14}H_{15}O_{11}$ is weakly bonded to its nearest neighbours. This is clearly seen in the fact that the inwarding H-bonds, such as $O_{11}-H_8$ and $O_{11}-H_{22}$ have the lengths 2.24 and 2.37 Å, respectively. The outwarding H-bond O_4-H_{14} is also strongly elongated to 2.21 Å. The angles $\angle O_5-H_8-O_{11} = 136.03^o$, $\angle O_4-H_{14}-O_{11} = 137.24^o$, and $\angle O_{11}-H_{22}-O_{19} = 129.83^o$ keep, therefore, a very low profile. The angle $\angle O_{11}-O_4-O_{19} = 63.95^o$ shows, in particular, a loss of tetrahedrality in this area of the pentacoordinated "patch". It seems worth discussing right now the distribution of oxygen-oxygen separations beyond the first coordination shell. They are quite well clustered around 4.65 Å and take the values: $R(O_4-O_{10}) = 4.32$ Å, $R(O_5-O_{19}) = 4.54$ Å, $R(O_4-O_{18}) = 4.62$ Å, $R(O_{19}-O_{21}) = 4.71$ Å, $R(O_{10}-O_{21}) = 4.84$ Å, $R(O_5-O_{21}) = 4.92$ Å, and $R(O_1-O_{11}) = 4.94$ Å. The oxygen atom is placed in a particularly privileged position because it stays very close to O_5 and O_{19}, namely, by 3.58 and 3.86 Å, respectively.

The dipole moment of the Defect II "patch" is very low and equal to 0.87 D. Energetically, it is situated 12.30 kcal/mol above the Ca structure. At room temperature, their difference in free energy is just 5.47 kcal/mol. Regarding the spectrum of this "patch", it is worth noting that the spectrum of Defect II possesses rather strong IR intensive bands. Namely, its most IR intensive and Raman active bands fall only in the region of stretching vibrations. This is the band $\nu_{28}^{H_2O} = 4113.9$ cm^{-1} with IR intensity 453.6 km/mol attributed chiefly to the stretching of O_1-H_3 bond. The second one, $\nu_{20}^{H_2O} = 3978$ cm^{-1}, with Raman activity 142.27 Å^4/amu and IR intensity 429.7 km/mol, is assigned to the composed symmetric stretching vibration of O_1-H_2 and $O_{18}-H_{16}$ bonds. From table 8 one can easily recognize the grouping of bands in the region 4091- 4168 cm^{-1} corresponding to the stretching vibrations of three O-H bonds which establish the five-fold coordination of the $H_6H_7O_4$ water molecule and of the other two directed to $H_{14}H_{15}O_{11}$. Comparing with the stretching modes of a water monomer, these bands are slightly redshifted, which indicates their weakness. This grouping of bands borders another one falling to 4205-4215 cm^{-1} and describing the stretching vibrations of unbonded or "free" O-H groups.

Table 8 also lists the most intensive vibrations of fully deuterated Defect II calculated at the HF/6-311G** level of computation. Its zero-point vibrational energy is 87.961 kcal/mol and entropy – 178.571 cal/mol·K.

Table 8. Most intensive bands of defect water octamer. For notations see caption of table 5. Values for fully deuterated Defect II are given in parenthesis.

No.	ν cm^{-1}	IR intensity	Raman activity	Force constant	Reduced mass Assignment
1	167.50 (139.68)	134.88 (66.82)	2.49 (0.13)	0.0217	1.3153 (2.4140)
		$O_{21}-H_{23}$			translation
2	186.88 (145.25)	188.76 (47.14)	0.82 (0.50)	0.0286	1.3893 (2.8709)
		$O_{18}-H_{20}$,	$O_{11}-H_{15}$		translation
3	454.54 (329.81)	247.97 (119.39)	1.45 (0.69)	0.1290	1.0594 (2.2083)
		$O_{19}-H_{22}$			libration
4	479.03 (347.03)	156.33 (94.76)	3.36 (1.69)	0.1426	1.0549 (2.1971)
		$O_{1}-H_{3}$,	$O_{19}-H_{22}$		libration
5	492.42 (357.49)	217.73 (108.48)	0.69 (0.39)	0.1513	1.0592 (2.2157)
		$O_{21}-H_{24}$,	$O_{19}-H_{22}$		libration
6	533.88 (387.10)	161.88 (114.83)	0.31 (0.43)	0.1781	1.0605 (2.1872)
		$O_{5}-H_{8}$,	$O_{11}-H_{14}$,	$O_{5}-H_{9}$	libration
7	546.94 (395.37)	170.08 (50.61)	3.40 (1.52)	0.1849	1.0492 (2.1872)
		$O_{4}-H_{7}$,	$O_{21}-H_{24}$		libration
8	601.84 (436.54)	202.77 (116.59)	1.35 (0.65)	0.2256	1.0571 (2.2097)
		$O_{5}-H_{9}$,	$O_{18}-H_{16}$		libration
9	654.55 (474.21)	134.04 (68.85)	0.87 (0.46)	0.2673	1.0591 (2.1829)
		$O_{5}-H_{9}$,	$O_{19}-H_{17}$		libration
10	668.36 (486.34)	332.08 (191.89)	1.49 (0.75)	0.2802	1.0646 (2.2347)
		$O_{18}-H_{16}$,	$O_{19}-H_{22}$		libration
11	693.47 (501.19)	250.72 (127.85)	0.93 (0.42)	0.2975	1.0501 (2.1782)
		$O_{19}-H_{17}$,	$O_{4}-H_{6}$		libration
12	757.18 (548.76)	149.08 (73.69)	1.94 (0.96)	0.3574	1.0582 (2.1919)
		$O_{4}-H_{6}$,	$O_{4}-H_{7}$		libration
13	798.45 (570.25)	381.95 (234.52)	0.13 (0.10)	0.3851	1.0488 (2.1742)
		$O_{1}-H_{2}$,	$O_{4}-H_{6}$,	$O_{10}-H_{13}$	libration
14	844.58 (615.41)	177.47 (112.25)	0.40 (0.13)	0.4484	1.0670 (2.2478)
		$O_{4}-H_{7}$,	$O_{1}-H_{2}$,	$O_{1}-H_{3}$,	
		$O_{21}-H_{24}-H_{18}$			libration
15	908.64 (654.81)	128.66 (77.92)	0.64 (0.30)	0.5079	1.0441 (2.1547)
		$O_{4}-H_{6}$,	$O_{19}-H_{17}$		libration
16	1754.08 (1282.64)	132.62 (67.93)	6.41 (3.41)	1.9589	1.0806 (2.2559)
		$O_{11}-H_{14}-H_{15}$			scissor
17	1774.04 (1295.89)	116.20 (54.80)	5.05 (2.71)	1.9991	1.0781 (2.2477)
		$O_{21}-H_{23}-H_{24}$			scissor
18	1843.89 (1344.61)	188.18 (100.98)	1.93 (1.11)	2.1503	1.0735 (2.2360)
		$O_{1}-H_{2}-H_{3}$,	$O_{5}-H_{8}-H_{9}$		scissor
19	3927.49 (2842.71)	257.45 (111.19)	122.55 (74.23)	9.6031	1.0566 (2.1797)
		$O_{4}-H_{6}$			stretch
20	3978.39 (2880.00)	429.69 (252.81)	142.27 (77.02)	9.8550	1.0568 (2.1812)
		$O_{1}-H_{2}$,	$O_{18}-H_{16}$		stretch
21	4003.26 (2897.42)	438.73 (199.00)	20.23 (11.63)	9.9717	1.0561 (2.1801)
		$O_{10}-H_{13}$,	$O_{18}-H_{16}$,	$O_{19}-H_{17}$	stretch
22	4015.09 (2903.59)	114.94 (48.68)	36.68 (19.66)	10.0101	1.0539 (2.1756)
		$O_{1}-H_{2}$,	$O_{18}-H_{16}$,	$O_{19}-H_{17}$	stretch
23	4034.36 (2917.34)	345.32 (143.67)	38.65 (19.40)	10.1096	1.0542 (2.1738)
		$O_{10}-H_{13}$,	$O_{19}-H_{17}$		stretch

Table 8. Continuation from previous page.

24	4058.52 (2937.93)	61.32 (36.05)	96.31 (40.38)	10.2950	1.0608 (2.1743)
		$O_{21}-H_{24}$,	O_4-H_7		stretch
25	4085.48 (2954.27)	426.88 (35.75)	35.90 (8.48)	10.5052	1.0682 (2.1656)
		O_4-H_7,	$O_{21}-H_{24}$		stretch
26	4091.03 (2955.79)	41.88 (53.56)	21.64 (45.36)	10.3624	1.0509 (2.1632)
		$O_{11}-H_{14}$,	O_5-H_9		stretch
27	4094.86 (2985.00)	48.83 (233.61)	67.66 (21.11)	10.3814	1.0508 (2.2772
		$O_{11}-H_{14}$,	O_5-H_9		stretch
28	4113.90 (3005.70)	453.56 (233.57)	37.92 (19.01)	10.6611	1.0692 (2.2742)
		O_1-H_3			stretch
29	4161.77 (3046.49)	96.49 (53.20)	26.93 (15.75)	11.0057	1.0785 (2.2812)
		O_5-H_8,	O_5-H_9,	$O_{19}-H_{22}$	stretch
30	4168.43 (3049.50)	256.07 (169.94)	23.34 (10.82)	11.0101	1.0755 (2.2797)
		$O_{19}-H_{22}$			stretch
31	4205.02 (3072.61)	104.06 (88.09)	49.36 (23.54)	11.1776	1.0729 (2.2705)
		$O_{10}-H_{12}$			stretch
32	4208.77 (3074.79)	100.10 (85.73)	52.66 (24.84)	11.1935	1.0725 (2.2691)
		$O_{18}-H_{20}$			stretch
33	4213.47 (3082.78)	116.91 (76.78)	43.67 (20.41)	11.2567	1.0762 (2.2801)
		$O_{21}-H_{23}$,	$O_{21}-H_{24}$		stretch
34	4214.21 (3087.05)	110.76 (88.40)	47.58 (19.72)	11.2964	1.0796 (2.2878)
		$O_{11}-H_{15}$,	$O_{11}-H_{14}$		stretch

Hence, the ratio $\mathrm{ZPVE}_{\mathrm{H_2O}}/\mathrm{ZPVE}_{\mathrm{D_2O}} = 1.53$ [27]. For the deuterium Defect II, the band $\nu_{20}^{\mathrm{D_2O}} = 2880.0$ cm^{-1} becomes most IR and most Raman active, simultaneously being contrary to the protium Defect II. We should also mention the behaviour of ν_{27} assigned to the coupled asymmetric stretching vibrations of $\mathrm{O}_{11}-\mathrm{H}_{14}$ and $\mathrm{O}_5-\mathrm{H}_9$ bonds under isotopic substitution. For the protium Defect II this band possesses IR intensity equal to 48.8 km/mol while it becomes five times more pronounced than its deuterated isotopomer. Analyzing the second and sixth columns of table 8 one finds that the calculated harmonic frequencies and reduced masses of the protium and deuterium Defect II do not show the known isotopic relationships connecting the ratio of frequencies of translational and bending modes $\nu^{\mathrm{H_2O}}/\nu^{\mathrm{D_2O}}$ with the square root of the ratio of the corresponding moments of inertia or masses, respectively. This is perhaps the common situation with computing harmonic vibrational frequencies [27], although, in our case with larger water clusters this deviation appears more pronounced than with water dimer. From table 8 it follows that, first, for $\nu_1^{\mathrm{H_2O}} = 167.5$ cm^{-1}, the ratio $\nu_1^{\mathrm{H_2O}}/\nu_1^{\mathrm{D_2O}} = 1.20$ whereas, according to this relationship, it should be $\sqrt{20/18} = 1.05$. Second, one directly obtains further that $\nu_2^{\mathrm{H_2O}}/\nu_2^{\mathrm{D_2O}} = 1.29$ and $\sqrt{\mu_2^{\mathrm{H_2O}}/\mu_2^{\mathrm{D_2O}}} = 1.44$. Third, for the rest of vibrations listed in table 8, the isotopic frequency ratios behave rather regularly around 1.37-1.38 with the exception for the 13th and 15th modes when they are 1.40 and 1.39, respectively. The isotopic reduced mass ratio does not reveal such a simple regularity, although it is largerly clustered near 1.44-1.45. Altogether, this isotopic analysis emphasizes a very anharmonic picture of the total potential energy surface of water clusters.

4. Summary

The fourteen different structures in the interval of 1.7 kcal/mol represent an unprecedentedly wide range of conformational excursions for water hexamer cluster. They illustrate how rich the picture of the total potential energy surface of liquid water might be.

The present work also provides the first *ab initio* demonstration of the pentacoordinated water hexamer structure. This structure is not, in fact, a defective one in the common sense of defects in the H-bonded pattern that violates the Bernal-Fowler-Pauling rules nor those structures that involve a bifurcated H-bond. It actually represents a novel structure of H-bonds where the approaching fifth water molecule forms a "dangling" bond with the central water molecule generating in such a way a pentacoordinated "patch" of higher density. This "patch", being incorporated into an H-bonded pattern of liquid water, on the one hand, partly contributes to nontetrahedral configurations and to the known blurred maximum of the O-O-O bond angle distribution function in the interval $60^o - 80^o$, in particular. On the other hand, it contributes to tetrahedral configurations as well. Notwithstanding that such hexamer and octamer five-fold coordinated "patches" occupy lower- lying local energetic minima on the total potential energy surfaces, they become energetically accessible at room temperature.

Acknowledgements

The author thanks Joel Bowman, Keiji Morokuma, and Jamal Musaev for many helpful discussions and hospitality. GAUSSIAN computing resources were provided by the Cherry L. Emerson Center for Scientific Computation at Emory University in Atlanta. The author also acknowledges stimulating discussions with Enrico Clementi, Gina Corongiu, Jens Peder Dahl, Ludwig Hofacker, Yves Marechal, Francesco Scortino, Georg Zundel, and Sotiris Xantheas. The author is grateful to Ihor Stasyuk for the inspiring scientific atmosphere and many useful discussions during his visits to Lviv.

References

1. (a)Eisenberg D., Kauzmann W. The structure and properties of water. Oxford, Clarendon, 1969; (b)F. Franks (Ed.) Water: a comprehensive treatise. New-York, Plenum, 1973. Vols.1-7, and References therein.
2. For Stasyuk's contribution to the hydrogen bond theory consult with: (a)Stasyuk I. V., Levitsky R. R. On elementary excitations in ferroelectrics with hydrogen bond. //Ukr. Fiz. Zh. 1969, vol 14, No 7, p.1097-1105; (b)Stasyuk I. V., Levitsky R. R. Coupled vibrations of a proton-ion system in ferroelectrics with hydrogen bonds of KH2PO4 type. //*Ibid.*, 1970, vol 15, No 3, p.460-469; (c)Stasyuk I. V., Levitsky R. R. The role of proton-phonon interaction in the phase transition of ferroelectrics with hydrogen bonds. //Phys. Stat.Sol.(b), 1970, vol 39, No 1, p.K35-K38; (d)Stasyuk I. V. Proton-phonon interaction in ferroelectrics with hydrogen bonds (strong coupling

approximation). //Teor. Mat. Fiz., 1971, vol 9, No 3, p.431-439; (e)Stasyuk I. V., Levitsky R. R. Dynamical theory of NH2H2PO4-type antiferroelectrics with hydrogen bonds. //Izv. Acad. Nauk SSSR, Ser. Fiz., 1971, vol 35, No 9, p.1775-1778; (f)Stasyuk I. V., Ivankiv A. L. Reduced set model for explanation of the molecular complexes with chains of hydrogen bonds. //Ukr. Fiz. Zh., 1991, vol 36, No 6, p.817-823; g)Stasyuk I. V., Stetsiv R. Y. Electronic states and optical effects in KH2PO4 type crystals with hydrogen bonds. //Izv. Acad. Nauk SSSR, Ser. Fiz., 1991, vol 55, No 3, p.522-525; (h)Stasyuk I. V., Ivankiv A. L. Thermodynamics of the molecular complexes with chains of hydrogen bonds. //Mod. Phys. Lett. B., 1992, vol 6, No 2, p.85-91; and References therein.

3. Bernal J. D., Fowler R. H. A theory of water and ionic solution, with particular reference to hydrogen and hydroxyl ions. //J. Chem. Phys., 1933, vol 1, No 8, p. 515-548; Pauling, L. The structure and entropy of ice and other crystals with some randomness of atomic arrangement. //J. Am. Chem. Soc., 1933, vol 57, No 7, p. 2680-2684.
4. (a)Rahman A., Stillinger F. H. Molecular dynamics study of liquid water. //J. Chem. Phys., 1971, vol. 55, No 7, p. 3336-3359; (b)Stillinger F. H., Rahman A. Improved simulation of liquid water by molecular dynamics. //*Ibid.*, 1974, vol. 60, No 4, p. 1545-1557.
5. (a)Geiger A., Stillinger F. H., Rahman A. Aspects of the percolation process for hydrogen-bond networks in water. //J. Chem. Phys., 1979, vol. 70, No 9, p. 4185-4193; (b)Mezei M., Beveridge D. L. Theoretical studies of hydrogen bonding in liquid water and dilute aqueous solutions. //*Ibid.*, 1981, vol. 74, No 1, p. 622-632.
6. (a)Stanley H. E., Teixeira J. Interpretation of the unusual behavior of H_2 O and D_2 O at low temperatures: tests of a percolation model. //J. Chem. Phys., 1980, vol. 73, No 7, p. 3404-3422; (b)Stanley H. E., Teixeira J., Geiger A., Blumberg R. L. Interpretation of the unusual behavior of H_2 O and D_2 O at low temperature: are concepts of percolation relevant to the "puzzle of liquid water" ? //Physica, 1981, vol. A 106, No 1, p. 260-277; (c)Geiger A., Stanley H. E. Low-density "patches" in hydrogen-bond network of liquid water: evidence from molecular-dynamics computer simulations. //Phys. Rev. Lett., 1982, vol. 49, No 24, p. 1749-1755; (d)Geiger A., Stanley H. E. Tests of universality of percolation exponents for a three-dimensional continuum system of interacting waterlike particles. //*Ibid.*, 1982, vol. 49, No 26, p. 1895-1898; (e)Blumberg R. L., Stanley H. E., Geiger A., Mausbach P. Connectivity of hydrogen bonds in liquid water. //J. Chem. Phys., 1984, vol. 80, No 10, p. 5230-5241; (f)Geiger A., Mausbach P. Molecular dynamics simulation studies of the hydrogen bond network in water. In J. C. Dore and J. Teixeira (Eds.), Hydrogen-bonded liquids, Dordrecht, Kluwer, 1991. pp 171-183.
7. (a)Luzar A., Chandler D. Structure and hydrogen bond dynamics of water-dimethyl sulfoxide mixtures by computer simulations. //J. Chem. Phys., 1993, vol. 98, No 10, p. 8160-8173; Effect of environment on hydrogen bond dynamics in liquid water. //Phys. Rev. Lett., 1996, vol. 76, No 6, p. 928-931; (b)Padró J. A., Martí J., Guàrdia E. Molecular dynamics simulation of liquid water at 523K. //J. Phys.: Condens. Matter, 1994, vol. 6, No 12, p. 2283-2290; (c)Martí J., Padró J. A., Guàrdia E. Molecular dynamics simulation of liquid water along the coexistence curve: hydrogen bonds and vibrational spectra. //J. Chem. Phys., 1996, vol. 105, No 2, p. 639-649.
8. (a)Narten A. H., Danford M. D., Levy H. A. X-ray diffraction study of liquid water

in the temperature range 4-200^o C. //Disc. Faraday Soc., 1967, vol. 43, p. 97-107; (b)Narten A. H., Levy H. A. Observed diffraction pattern and proposed models of liquid water. //Science, 1969, vol. 165, No 3892, p. 447-454; (c)Soper A. K., Phillips M. G. A new determination of the structure of water at 25^o C. //Chem. Phys., 1986, vol. 107, No 1, p. 47-60; (d)Narten A. H., Levy H. A. Atom-pair distribution function of liquid water at 25^o C from neutron diffraction. //Science, 1982, vol. 217, No 4564, p. 1033-1035; (e)Morgan J., Warren B. E. X-ray analysis of the structure of water. //J. Chem. Phys., 1938, vol. 6, No 9, p. 666-673. See also: Cho C. H., Singh S., Robinson G. W. An explanation of the density maximum in water. //Phys. Rev. Lett., 1996, vol. 76, No 10, p. 1651-1654.

9. Giguére P. A. Bifurcated hydrogen bonds in water. //J. Raman Spectrosc., 1984, vol. 15, No 5, p. 354-359; The bifurcated hydrogen-bond model of water and amorphous ice. //J. Chem. Phys., 1987, vol. 87, No 8, p. 4835-4839.
10. (a)Walrafen G. E., Hokmabadi M. S., Yang W.-H., Chu Y., Monosmith W. B. Collision-induced Raman scattering from water and aqueous solutions. //J. Phys. Chem., 1989, vol. 93, No 8, p. 2909-2917; (b)Walrafen G. E., Hokmabadi M. S., Yang W.-H. Raman investigation of the temperature dependence of the bending ν_2 and combination $\nu_2 + \nu_L$ bends from liquid water. //*Ibid.*, 1988, vol. 92, No 9, p. 2433-2438; (c)Walrafen G. E. Raman spectrum of water: transverse and longitudinal acoustic modes below $\approx$ 300cm^{-1} and optic modes above $\approx$ 300cm^{-1}. //*Ibid.*, 1990, vol. 94, No 6, p. 2237-2239.
11. (a)Bjerrum N. Structure and properties of ice. //K. Danske Vid. Selsk. Mat.-Fys. Medd., 1951, vol. 27, No 1, p. 3-56; Structure and properties of ice. //Science, 1952, vol. 115, No 2989, p. 385-390; (b)Originally from the German word "leer" that means "empty"; (c)Originally from the German word "doppelt" that means "double".
12. (a)Dunitz J. D. Nature of orientational defects in ice. //Nature, 1963, vol. 197, No 4870, p. 860-862; (b)Cohan N. V., Cotti M., Iribarne J. V., Weissmann M. Electrostatic energies in ice and the formation of defects. //Trans. Faraday Soc., 1962, vol. 58, No 471, p. 490-498; (c)Eisenberg D., Coulson C. A. Energy of formation of D-defects in ice. //Nature, 1963, vol. 199, No 4891, p. 368-369; (d)Kavanau J. L. Structure and function in biological membranes. San Francisco, Holden-Day, 1965. Vol. I, p. 175ff; (e)Newton M. D. Small water clusters as theoretical models for structural and kinetic properties of ice. //J. Phys. Chem., 1983, vol. 87, No 21, p. 4288-4292; (f)Newton M. D., Jeffrey G. A., Takagi S. Application of ab initio molecular orbital calculations to the structural moieties of carbohydrates. 5. The geometry of the hydrogen bonds. //J. Am. Chem. Soc., 1979, vol. 101, No 18, p. 1997-2002; (g)Jeffrey J. A., Saenger W. Hydrogen bonding in biological structures. Berlin, Springer, 1991. p. 20ff; (h)Head-Gordon M., Head-Gordon T. Analytic MP2 frequencies without fifth-order storage. Theory and application to bifurcated hydrogen bonds in the water hexamer. //Chem. Phys. Lett., 1994, vol. 220, Nos 1,2, p. 122-128.
13. (a)Kryachko E. S. The cooperative model for orientational defects in ice: continuum approximation. //Chem. Phys. Lett., 1987, vol. 141, No 2, p. 346-349; Collective model of orientational defect in ice within the continuum approach. //Solid State Phys. (USSR), 1987, vol. 29, No 2, p. 345-350; (b)Yanovitskii O. E., Kryachko E. S. Model for orientational defects in quasi-one-dimensional ice crystals. //Phys. Stat. Sol. (b), 1988, vol. 147, No 1, p. 69-81; (c)Kryachko E. S. Recent developments in solitonic model of proton transfer in quasi-one-dimensional infinite hydrogen-bonded systems.

In A. Müller, H. Ratajczak, W. Junge, and E. Diemann (Eds.), Electron and proton transfer in chemistry and biology. Amsterdam, Elsevier, 1992. pp. 363-385.
14. Devlin J. P. Vibrational spectra and point defect activities of icy solids and gas phase clusters. //Int. Rev. Phys. Chem., 1990, vol. 9, No 1, p. 29-65; Fisher M., Devlin J. P. Defect activity in amorphous ice from isotopic exchange data: insight into the glass transition. //J. Phys. Chem., 1995, vol. 99, No 29, p. 11584-11590.
15. Prielmeier F. X., Lang E. W., Lüdemann H. D., Speedy R. J. Diffusion in supercooled water to 300 MPa. //Phys. Rev. Lett., 1987, vol. 59, No 10, p. 1128-1131.
16. Geiger A., Mausbach P., Schnitker J. Computer simulation study of the hydrogen-bond network in metastable water. In G. W. Neilson and J. E. Enderby (Eds.), Water and aqueous solutions. Bristol, Adam Hilger, 1986; pp. 15-30.
17. (a)Sciortino F., Geiger A., Stanley H. E. Network defects and molecular mobility in liquid water. //J. Chem. Phys., 1992, vol. 96, No 5, p. 3857-3865; (b)Sciortino F., Geiger A., Stanley H. E. Isochoric differential scattering functions in liquid water: the fifth neighbor as a network defect. //Phys. Rev. Lett., 1990, vol. 65, No 27, p. 3452-3455.
18. Head-Gordon T., Stillinger F. H. An orientational perturbation theory for pure liquid water. //J. Chem. Phys., 1993, vol. 98, No 4, p. 3313-3327. See Figs. 5 and 20 in particular.
19. (a)Jedlovszky R., Bakó I., Pálinkás G., Radnai T., Soper A. K. Investigation of the uniqueness of the reverse Monte Carlo method: studies on liquid water. //J. Chem. Phys., 1996, vol. 105, No 1, p. 245-254; (b)Bruni F., Ricci M. A., Soper A. K. Unpredicted density dependence of hydrogen bonding in water found by neutron diffraction. //Phys. Rev., 1996, vol. B 54, No 17, p. 11876-11879.
20. GAUSSIAN 94, Revision B.3, M. J. Frisch, G. W. Trucks, H. B. Schlegel, P. M. W. Gill, B. G. Johnson, M. A. Robb, J. R. Cheeseman, T. Keith, G. A. Petersson, J. A. Montgomery, K. Raghavachari, M. A. Al-Laham, V. G. Zakrzewski, J. V. Ortiz, J. B. Foresman, C. Y. Peng, P. Y. Ayala, W. Chen, M. W. Wong, J. L. Andres, E. S. Replogle, R. Gomperts, R. L. Martin, D. J. Fox, J. S. Binkley, D. J. Defrees, J. Baker, J. P. Stewart, M. Head-Gordon, C. Gonzalez, and J. A. Pople, Gaussian, Inc., Pittsburgh, PA, 1995.
21. (a)Krishnan R., Binkley J. S., Seeger R., Pople J. A. Self-consistent molecular orbital methods. XX. A basis set for correlated wave functions. //J. Chem. Phys., 1980, vol. 72, No 1, p. 650-654; (b)Frisch M. J., Pople J. A., Binkley J. S. Self-consistent molecular orbital methods 25. Supplementary functions for Gaussian basis sets. //*Ibid.*, 1984, vol. 80, No 7, p. 3265-3269.
22. (a)Xantheas S. S., Dunning T. T., Jr. *Ab initio* studies of cyclic water clusters $(H_2 O)_n$, n=1-6. I. Optimal structures and vibrational spectra. //J. Chem. Phys., 1993, vol. 99, No 11, p. 8774-8792; (b)Xantheas S. S. *Ab initio* studies of cyclic water clusters $(H_2 O)_n$, n=1-6. II. Analysis of many-body interactions. //*Ibid.*, 1994, vol. 100, No 10, p. 7523-7534; (c)Tsai C. J., Jordan K. D. Theoretical study of the $(H_2 O)_6$ cluster. //Chem. Phys. Lett., 1993, vol. 213, Nos 1, 2, p. 181-188; (d)Krishnan P. N., Jensen J. O., Burke L. A. Theoretical studies of water clusters. II. Hexamer. //*Ibid.*, 1994, vol. 217, No 3, p. 311-318; (e)Estrin D. A., Paglieri L., Corongiu G., Clementi E. Small clusters of water molecules using density functional theory. //J. Phys. Chem., 1996, vol. 100, No 21, p. 8701-8711.
23. (a)Jensen J. O., Krishnan P. N., Burke L. A. Theoretical study of water clusters:

octamer. //Chem. Phys. Lett., 1995, vol. 246, Nos 1, 2, p. 13-19; (b)Kim J., Mhin B. J., Lee S. J., Kim K. S. Entropy-driven structure of the water octamer. //*Ibid.*, 1994, vol. 219, Nos 3, 4, p. 243-246; (c)Knochenmuss, R., Leutwyler S. Structure and vibrational spectra of water clusters in the self-consistent-field approximation. //J. Chem. Phys., 1992, vol. 96, No 7, p. 5233-5244; (d)Kim K., Jordan K. D., Zwier T. S. Low-energy structures and vibrational frequencies of the water hexamer: comparison with benzene-$(H_2\,O)_6$. //J. Am. Chem. Soc., 1994, vol. 116, No 25, p. 11568; (e)Liti K., Brown M. G., Carter C., Saykally R. J., Gregory J. K., Clary D. C. Characterization of a cage form of the water hexamer. //Nature, 1996, vol. 381, No 6582, p. 501-503; (f)Gregory J. K., Clary D. C. Structure of water clusters. The contribution of many-body forces, monomer relaxation, and vibrational zero-point energy. //J. Phys. Chem., 1996, vol. 100, No 46, p. 18014-18022; (g)Liu, K., Brown M. G., Saykally R. J. Terahertz laser vibration-rotation tunneling spectroscopy and dipole moment of a cage form of the water hexamer. //*Ibid.*, 1997, vol. A 101, No 27, p. 8995-9010.

24. (a)Mills I. M. Harmonic and anharmonic force field calculations. In R. N. Dixon (Ed.), Theoretical chemistry. London, Chemical Society, 1974. Vol. 1-Quantum Chemistry, p. 110-159; (b)Honegger E., Leutwyler S. Intermolecular vibrations of small water clusters. //J. Chem. Phys., 1988, vol. 88, No 4, p. 2582-2595, Table II and Refs. therein. Experimental harmonic frequencies of water molecule are the following: $\nu_1^{expt} = 3832$ cm^{-1}, $\nu_2^{expt} = 1649$ cm^{-1}, and $\nu_3^{expt} = 3942$ cm^{-1}; (c)$\nu_2^{theor} =$ 1750.30 cm^{-1} at the HF/6-311G** level; (d)Scaling factors $f_i = \nu_i^{theor}/\nu_i^{expt}, i = 1,2,3$ are equal to 1.0809, 1.0614, 1.0750, respectively. The average scaling factor $< f >= (f_1 + f_2 + f_3)/3 = 1.0724$; (e)The scaled frequencies $\nu_i^{sca} = \nu_i^{theor}/ < f >$ (with the relative error, $\delta = (\nu_i^{sca} - \nu_i^{expt})/\nu_i^{expt}, \%$) are 3862.17 $cm^{-1}(+0.79\%), 1632.09\mathrm{cm}^{-1}(-1.03\%), 3951.43\mathrm{cm}^{-1}(+0.21\%)$.

25. The relative properities of Defect II with respect to the R6c structure are: ΔE = 2 $\cdot 10^{-4}$ kcal/mol, ΔH = - 4 $\cdot 10^{-4}$ kcal/mol, and ΔS = - 21.74 cal/mol·K.

26. For instance, the frequencies ν and reduced masses μ of water isotopomers H_2O and D_2O calculated via STO-3G basis set are the following: $\nu_1^{H_2O(D_2O)} = 4142.29$ (2992.49) cm^{-1}, $\mu_1^{H_2O(D_2O)} = 1.0491$ (2.1747) amu; $\nu_2^{H_2O(D_2O)} = 2169.80$ (1584.65) cm^{-1}, $\mu_2^{H_2O(D_2O)} = 1.0785$ (2.2429) amu; and $\nu_3^{H_2O(D_2O)} = 4393.38$ (3212.88) cm^{-1}, $\mu_3^{H_2O(D_2O)} = 1.0774$ (2.2696) amu. Further, ZPVE$_{H_2O}$ = 15.30 kcal/mol, ZPVE$_{D_2O}$ = 9.94 kcal/mol, and their ratio ZPVE$_{H_2O}$/ZPVE$_{D_2O}$ = 1.54. Also, $\nu_1^{H_2O}/\nu_1^{D_2O} = 1.38$, $\nu_2^{H_2O}/\nu_2^{D_2O} = \nu_3^{H_2O}/\nu_3^{D_2O} = 1.37$, and $\sqrt{\mu_1^{H_2O}/\mu_1^{D_2O}} = \sqrt{\mu_2^{H_2O}/\mu_2^{D_2O}} = 1.44$, $\sqrt{\mu_3^{H_2O}/\mu_3^{D_2O}} = 1.45$.

27. We analyze the ratio ν^{H_2O}/ν^{D_2O} for the harmonic vibrational frequencies of water dimer calculated in [28] at the HF/6-31G* and MP2 levels. Following Tables 1 and 2 of [28], one easily derives that this ratio spans the range 1.16-1.18 for all listed modes.

28. Scheiner S., Čuma M. Relative stability of hydrogen and deuterium bonds. //J. Am. Chem. Soc., 1996, vol. 118, No 6, p. 1511-1521.

Ab initio гексамери і октамери води: знаряддя до вивчення водневозв'язаних кластерів у рідкій воді

Є.Крячко [1,2,3]

[1] Інститут теоретичної фізики ім. М.М.Боголюбова,
252143 м. Київ-143, вул. Метрологічна, 14б

[2] Центр наукових обчислень Черрі Л. Емерсона і Відділення хімії Університету Еморі, Атланта, GA 30322, США

[3] Університет Джона Хопкінса, Відділення хімії,
Балтімор, MD 21218, США

Отримано 18 березня 1998 р.

Чотирнадцять різних структур гексамера води, які знайдені методом *ab initio* в базисі 6-311G** в інтервалі 1.7 kcal/mol вище глобального мінімуму, є безпрецедентним прикладом високої конформаційної пластичності рідкої води. Дана робота також вперше демонструє існування пентакоординаційних кластерів води на рівні прецизійних *ab initio* розрахунків.

Ключові слова: *рідка вода, Н-зв'язаний комплекс, орієнтаційний дефект, водний кластер, "гойдальний" зв'язок, ab initio HF 6-311** обчислення*

PACS: *61.20.Ja, 61.25.Em, 61.20.Gy, 62.30.+d, 63.20.Pw, 63.90.+t, 64.70.Ja, 65.50.+m, 64.30.+t*